ESC HEART FAILURE
ESC Heart Failure (2024)
Published online in Wiley Online Library (wileyonlinelibrary.com) **DOI:** 10.1002/ehf2.15050

ORIGINAL ARTICLE

Integrin beta-like 1 is regulated by DNA methylation and increased in heart failure patients

Lauren Kerrigan[1], Kevin Edgar[1], Adam Russell-Hallinan[1], Oisin Cappa[1], Nadezhda Glezeva[2], Carlos Galan-Arriola[3], Eduardo Oliver[3], Borja Ibanez[3], John Baugh[2], Patrick Collier[4], Mark Ledwidge[2], Ken McDonald[2], David Simpson[1], Sudipto Das[5], David J. Grieve[1] and Chris J. Watson[1]*

[1]*Wellcome-Wolfson Institute for Experimental Medicine, Queen's University Belfast, Belfast, UK;* [2]*UCD Conway Institute and Research and Innovation Programme for Chronic Disease, School of Medicine, University College Dublin, Dublin, Ireland;* [3]*Centro Nacional de Investigaciones Cardiovasculares (CNIC), Madrid, Spain;* [4]*Department of Cardiovascular Medicine, Cleveland Clinic, Cleveland, Ohio, USA; and* [5]*Royal College of Surgeons, Dublin, Ireland*

Abstract

Aims Dynamic alterations in cardiac DNA methylation have been implicated in the development of heart failure (HF) with evidence of ischaemic heart disease (IHD); however, there is limited research into cell specific, DNA methylation sensitive genes that are affected by dysregulated DNA methylation patterns. In this study, we aimed to identify DNA methylation sensitive genes in the ischaemic heart and elucidate their role in cardiac fibrosis.

Methods A multi-omics integrative analysis was carried out on RNA sequencing and methylation sequencing on HF with IHD (n = 9) versus non-failing (n = 9) left ventricular tissue, which identified Integrin beta-like 1 (*ITGBL1*) as a gene of interest. Expression of *Itgbl1* was assessed in three animal models of HF; an ischaemia-reperfusion pig model, a myocardial infarction mouse model and an angiotensin-II infused mouse model. Single nuclei RNA sequencing was carried out on heart tissue from angiotensin-II infused mice to establish the expression profile of *Itgbl1* across cardiac cell populations. Subsequent *in vitro* analyses were conducted to elucidate a role for *ITGBL1* in human cardiac fibroblasts. DNA pyrosequencing was applied to assess *ITGBL1* CpG methylation status in genomic DNA from human cardiac tissue and stimulated cardiac fibroblasts.

Results *ITGBL1* was >2-fold up-regulated (*FDR adj P* = 0.03) and >10-fold hypomethylated (*FDR adj P* = 0.01) in human HF with IHD left ventricular tissue compared with non-failing controls. Expression of *Itgbl1* was up-regulated in three isolated animal models of HF and showed conserved correlation between increased *Itgbl1* and diastolic dysfunction. Single nuclei RNA sequencing highlighted that *Itgbl1* is primarily expressed in cardiac fibroblasts, while functional studies elucidated a role for *ITGBL1* in cardiac fibroblast migration, evident in 50% reduced 24 h fibroblast wound closure occurring subsequent to siRNA-targeted *ITGBL1* knockdown. Lastly, evidence provided from DNA pyrosequencing supports the theory that differential expression of *ITGBL1* is caused by DNA hypomethylation.

Conclusions *ITGBL1* is a gene that is mainly expressed in fibroblasts, plays an important role in cardiac fibroblast migration, and whose expression is significantly increased in the failing heart. The mechanism by which increased *ITGBL1* occurs is through DNA hypomethylation.

Keywords Heart failure; Ischaemic cardiomyopathy; Epigenetics; DNA methylation; Single nuclei RNA sequencing: cardiac fibroblasts

Received: 22 April 2024; Revised: 17 July 2024; Accepted: 21 August 2024
**Correspondence to: Chris Watson, Wellcome-Wolfson Institute for Experimental Medicine, Queen's University, 97 Lisburn Rd, Belfast BT9 7BL, USA.*
E-mail: chris.watson@qub.ac.uk

Introduction

Cardiomyopathy, a word that literally translates as 'disease of the heart muscle', is a general term describing a range of alterations to cardiac cells which manifest in structural and functional myocardial abnormalities, in the absence of coronary artery disease, hypertension, valvular disease, and congenital heart disease, that ultimately result in heart failure (HF).[1] Cardiomyopathies can be genetic, acquired or a combination of both, can coexist with ischaemic, valvular

or hypertensive disease, and are associated with considerable morbidity and mortality.[1] Ischemic heart disease (IHD) is currently the most common cause of HF in the developed world.[2] Significant advances in treatment of patients who have suffered acute myocardial infarction have enhanced the predominance of HF secondary to IHD. IHD affects approximately 126 million individuals worldwide, and around 9 million deaths per year are associated with IHD, making it the leading cause of mortality.[3] It has retained this position for the past two decades, and its prevalence is only predicted to increase given the ongoing rise in obesity, diabetes and the ageing population.

Unremitting myocardial ischaemia, due to impaired epicardial blood flow and/or coronary flow reserve, augments a milieu of pathophysiological mechanisms, including neurohumoral changes, excessive inflammation and propagated fibrosis, resulting in diminished left ventricular (LV) systolic function.[4] It has been established that aberrant transcriptional regulation in cardiac cells, including cardiomyocytes (CMs), cardiac fibroblasts (CFs), endothelial cells and inflammatory cells, are attributed to the development of HF with IHD aetiology.

DNA methylation is an important epigenetic regulatory mechanism that controls transcriptional gene expression; irregular changes to DNA methylation patterns in cardiac cell populations have been shown to play a role in maladaptive cardiac remodelling in HF with IHD, as well as occurring as a consequence of the disease.[5,6] In a study carried out by us in 2019, methylation signatures in cardiac tissue from HF patients with evidence of IHD were identified as potential biomarkers and/or therapeutic targets, however the functional impact of these specific dysregulated genes were not fully elucidated.[7]

In this study, we aimed to identify specific DNA methylation sensitive genes in LV tissue from HF patients with IHD through integrated use of targeted bisulfite sequence capture sequencing and RNA sequencing. Through this work, integrin beta-like 1 (*ITGBL1*) was identified as a candidate gene of interest and is the focus of this study.

Methods

Human interventricular septal tissue (IVS)

This study conformed to principles outlined in the Declaration of Helsinki. Ethical Approval for data collection and use of tissue was obtained from the Cleveland Clinic Institutional Review Board and all subjects gave written informed consent to participate. Cardiac IVS tissue was surgically extracted from patients with HF with evidence of IHD who underwent orthotropic cardiac transplantation (OCT) (n = 9). IVS from non-failure (NF) patients who died of non-cardiac causes with no known history of HF were collected as an age-matched (45–60 years) and gender-matched (all males) control group (n = 9). Patient characteristics for these groups have been previously reported[7] and are summarized in *Table* S1. Excised cardiac tissue was snap frozen in liquid nitrogen and stored at −80°C until required.

Methylation sequencing

Custom-designed next generation targeted methylation sequencing was previously performed on genomic DNA isolated from cardiac tissue from HF patients with IHD and matched control patients. Detailed description of methods is provided in a previous study publication.[7]

RNA sequencing of patient cardiac tissue

Approximately 30 mg of IVS tissue was physically homogenized by a motorized pellet pestle (Sigma-Aldrich). Total RNA was extracted from tissue homogenate using RNeasy Fibrous Tissue Mini Kit (Qiagen) following manufacturer's instructions. To confirm presence of RNA, samples were quantified using the Qubit™ RNA Assay Kit (Thermo Fisher).

Library preparation and next-generation sequencing were carried out by the Queen's University Belfast Genomics Core Technology Unit. Libraries were prepared from 1 μg of RNA using TruSeq® Stranded mRNA Library Prep kit (Illumina) following the manufacturer's instructions. Library concentrations were measured using Qubit™ dsDNA HS Assay Kit (Thermo Fisher). Quality and concentration of libraries were determined by Fragment Analyzer (Advanced Analytical). Libraries were sequenced on a NextSeq 500 System (Illumina).

An analytical workflow on CLC Genomics workbench v10.1.1 (QIAGEN) was used for sequence analyses. Imported raw sequence fastq files were assessed for QC, trimmed and extracted; reads were then mapped to HG19. Mature annotated sequences were assigned experimental groups (NF v HF with IHD). Gene mapping matrices were normalized to RPMM and compared between experimental groups for differential gene expression. Proportion based statistical analysis (Baggerly's test, Bonferroni corrected) was also carried out on the CLC Genomics workbench package.

Animal studies

This investigation conforms to the *Guide for the Care and Use of Laboratory Animals* published by the US National Institutes of Health (NIH Publication No. 85-23, revised 1985).

Porcine model of Ischaemia-reperfusion cardiac injury

Ischaemia was induced in 3 month old, large white male pigs by inflating an angioplasty balloon in the mid-portion of the left anterior descending (LAD) coronary artery, occluding the LAD immediately distal to the origin of the first diagonal branch. At the end of the pre-specified ischaemia duration (40–50 min), animals were reperfused (balloon deflation) and recovered from anaesthesia (n = 8). Further details of sedation, analgesia and surgery are outlined in Supporting information methods. The control group consisted of healthy pigs which did not undergo an angioplasty balloon inflation of the LAD coronary artery (n = 5). LV volumes and LV ejection fraction (LVEF) were assessed by cardiac magnetic resonance (CMR) imaging 45 days after infarction induction. Animals were euthanized and hearts were excised.

CMR imaging

Cine and contrast-enhanced CMR studies were performed 7 and 45 days after MI induction. CMR examinations were conducted using a Philips 3-T Achieva Tx whole body scanner (Philips Healthcare, Best, the Netherlands) equipped with a 32-element phased-array cardiac coil. The imaging protocol included a standard segmented cine steady-state free-precession sequence to provide high-quality anatomic references and assessment of LVEF. LV volumes were normalized to body surface area according to Brody's formula and CMR images were evaluated with dedicated software (MR Extended Work Space 2.6; QMassMR 7.6; Medis, Leiden, the Netherlands) by two observers experienced in CMR analysis and blinded to group allocation.

Murine chronic coronary artery ligation model of myocardial infarction

MI was induced in 12-week-old, female C57Bl/6 mice by passing a 7–0 suture under the LAD coronary artery and permanently tying using a single uninterrupted suture. After ligation, blanching of the myocardium was visualized. Following surgery, mice were recovered from anaesthesia and placed in a recovery cage at 37°C for 10–15 min, then housed in a heated room at 26°C for the duration of the study where they were observed routinely for signs of pain or distress. Further details of sedation, analgesia and surgery are outlined in supporting information methods. The control group consisted of animals that had been sedated and had the chest and thoracic cavity exposed but did not have the LAD artery ligated (sham). An endpoint echocardiogram was carried out; animals were euthanized and hearts excised at 7 days post ligation. The apex of the LV was fixed for histological analysis, remaining LV was stored for further gene expression and protein expression analysis.

Murine model of angiotensin-II induced hypertension

Male 8 week old C57Bl/6 mice were anaesthetized, a small incision was made in the left flank of the animal and an osmotic minipump (Alzet pumps, Charles River) containing either saline or angiotensin II (Ang II) (Bachem) was inserted into a pocket of tissue in the subdermal space. Mice were observed for 72 h to assess general welfare and wound healing. Further details of sedation, analgesia and surgery are outlined in supporting information methods. Mice received 1.5 mg/kg/day Ang II, and control mice received saline, via osmotic minipump for a total of 4 weeks. Systolic blood pressure was measured routinely throughout the study (endpoint systolic blood pressure measurements presented in supporting information methods). An endpoint echocardiogram was carried out, then animals were humanely euthanized and LV heart tissue was excised. The apex of the LV was fixed for histological analysis, remaining LV was stored for further gene expression and protein expression analysis.

Echocardiographic measurement

Endpoint echocardiography was used to assess LV structure and function in animals anesthetized using 1.5% isoflurane. Echocardiography was performed using a Vevo770 system (VisualSonics) equipped with a 55 MHz ultrasound transducer. Two-dimensional images were captured in LV parasternal long axis and parasternal short axis. LVEF and LV posterior wall thickness (LVPW) were calculated using images obtained by LV M-mode tracing. isovolumic relaxation time (IVRT) was calculated using images obtained by Doppler-mode imaging.

Histological assessment of collagen deposition

Paraffin-embedded heart tissue was sectioned, mounted on to a glass microscopy slide and stained with picrosirius red to assess cardiac interstitial collagen deposition. In brief, tissue sections were exposed to xylene and a series of graded alcohols (100%, 95%, 70% and 50%) for 3 min per grade, then submerged in distilled water for 5 min to stimulate tissue affinity for the dye. Slides were then immersed in 0.2% phosphomolybdic acid (Fluka Analytical, Poole, UK) for 2 min and rinsed in distilled water before immersion in 0.1% picrosirius red (Direct Red 80 in saturated Picric Acid; Fluka Analytical, Poole, UK) for 1 h. Slides were washed in acidified water (0.5% v/v acetic acid in distilled water) for

2 min before dehydration through graded alcohols (50%, 75% and 100%), 1 min per grade. Finally, slides were cleared in xylene and a coverslip applied with DPX mounting medium. Cardiac collagen deposition was then quantified in whole tissue section images (Lica AT2 scanner), by blinded digital image analysis using ImageScope® software.

Nuclei isolation

Single-nuclei cardiac isolations were prepared using murine whole heart tissue harvested from Ang II-induced hypertensive mice according to a protocol modified from McLellan et al.[8] Briefly, excised hearts were dissected to remove the atria and right ventricle. The LV was minced, then dissociated into a cell suspension enzymatic digestion (Collagenase II 600 U/mL and DNase I 6 U/mL). Undigested tissue was excluded using 250 μm strainers, followed by red blood cell lysis and debris clean-up. Nuclei isolation was achieved through the use of a hypotonic solution to swell cells, followed by mechanical fragmentation by passing through a 30-gauge hypodermic needle. To achieve the desired nuclei suspension concentration for 10× Single-Nuclei sequencing, nuclei from three hearts per condition were pooled into single nuclei suspensions, then loaded in the 10× Chromium platform to achieve cDNA libraries of approximately 2000 nuclei per pooled suspension.

Data processing

Single-nuclei cDNA libraries were sequenced with the Illumina NextSeq P2 platform. 10× Genomics Cellranger (6.0.2) was used to process raw sequencing data. Sample pools were demultiplexed into fastq format with Cellranger mkfastq, followed by alignment against the mm10 reference genome package using Cellranger count to generate gene expression matrices.

SoupX

R package SoupX v1.6.17 was used to profile and normalize for ambient mRNA contamination detected in pooled sample libraries. Briefly, count data assigned to non-cell barcode ID were profiled to characterize ambient mRNA for each nuclei suspension, arising largely from haemoglobin and mitochondrial transcripts originating in lysed cells. Such transcripts in suspension are commonly co-captured with cells/nuclei in droplet-based single-cell/nuclei platforms and may influence results if not corrected. Using SoupX, expression of genes disproportionately contributing to the ambient mRNA profile was reduced by a commensurate amount for each QC-passing barcode ID determined algorithmically to represent a single nucleus.

Single-nuclei QC and clustering

After ambient mRNA correction, filtered matrices were analysed in R (v4.2.1) using Seurat v4.1.18. For each library, a further QC step was performed to remove genes expressed in less than 3 nuclei, and nuclei with fewer than 500 counts or with >50% counts mapping to mitochondrial genes. An initial round of clustering identified a cluster of nuclei disproportionately affected by haem/MT expression, which were excluded from analysis, resulting in a final filtered dataset of 4395 QC-passing nuclei. The dataset was scaled to regress out variation attributed to mitochondrial and ribosomal transcripts, after which a final round of clustering was performed.

Single-nuclei gene expression analysis

Marker genes were detected for each cluster in Seurat using the MAST package (version 1.12.09), enabling manual cell type annotation based on canonical marker gene expression. Differential expression testing between treatments was performed in Seurat using default parameters, with changes of log2 fold-change ≥ 0.5 and adjusted P value < 0.05 accepted as significantly altered gene expression.

Co-expression correlation analysis was performed in R to determine genes correlated in expression with *ITGBL1* in cardiac fibroblasts. The cor.test function was applied using Kendall's tau statistic to calculate and rank statistically significant correlations, with correlations of tau greater than 0.15 or less than −0.15, and adjusted P value of <0.05 considered significantly correlated. Genes with significant positive correlation were submitted to EnrichR[9] for gene set enrichment using NCATS BioPlanet database.[10]

Cell culture

Primary human cardiac fibroblasts (HCFs) were purchased from ScienCell Research Laboratories; sourced from two individual donors. Cells were cultured and maintained in Dulbecco modified Eagle medium (DMEM; Gibco), supplemented with 10% foetal bovine serum (Gibco) in a 21%O2, 5% CO2 humidified incubator at 37°C. Cells were not expanded beyond 15 population doublings in line with suggested conditions provided by ScienCell Research Laboratories. In hypoxia exposure experiments, HCFs were cultured in a 1%O2, 5%CO2 humidified hypoxic chamber at 37°C. In transforming growth factor (TGF) stimulation experiments, HCF cells were treated for 72 h with either vehicle or 5 ng/mL human recombinant TGF-β1 (Promokine) in serum free media. Human CMs (AC16s) were cultured in Dulbecco's Modified Eagle Medium: Nutrient Mixture F-12 (DMEM/F12; Gibco) supplemented with 10% foetal bovine serum (Gibco) in a 21% O_2, 5% CO_2 humidified incubator at 37°C.

In Ang II stimulation experiments, AC16 cells were treated for 72 h with either vehicle or 25 nM Ang II. Supernatants from these experiments were collected. Media was prepared in a 1:3 mixture of either DMEM:AC16 + Ang II supernatant, DMEM:AC16vehicle supernatant or cell-free DMEM:DMEM F-12 containing Ang II that was incubated at 37°C for 72 h. HCFs were cultured in these media/supernatant mixtures for 24 h.

Cell transfection and migration assay

HCFs were maintained under normal culture conditions and transfected with 20 nM *ITGBL1* siRNA (Horizon Inc) or 20 nM non-targeting siRNA (Scr). HCFs were then treated with either vehicle or 5 ng/mL human recombinant TGF-β1 (Promokine). For scratch wound assays, a scratch was performed in a vertical line down each well using a blunt 20 μL pipette tip prior to treatment. At 48 h post-transfection, images were captured and cell pellets were collected for RNA and protein analysis. For migration assays, HCFs were cultured in 24 well dishes containing Radius© 24-well migration assay 0.68 μM biocompatible gels (Generon). HCF cells were transfected; 24 h post-transfection migration gels were removed exposing the cell-free area for migration. At 24 h post gel removal, cells were washed and stained with calcein for 30 min before imaging. Detailed description of cell transfection, treatments and assays are outlined in supporting information methods.

Western blotting

Protein expression levels were measured by western blotting on lysates prepared from HCF cells and human/murine/porcine LV tissue. Cells were lysed in RIPA lysis buffer and LV tissue was mechanically homogenized in RIPA lysis buffer using a motorized pellet pestle (Sigma-Aldrich). Protein concentrations were measured by BCA protein assay (Promega). Protein lysates (30–50 μg) were electrophoresed on 12% sodium dodecyl sulfate-polyacrylamide gels and then transferred onto polyvinylidene fluoride (PVDF) membranes (BioRad) using a gel transfer device. PVDF membranes were blocked in 5% non-fat milk/*tris*-buffered saline with 0.01% Tween™ 20 (TBS-T) for 1 h and then incubated with primary antibodies against ITGBL1 (Abcam, 1:1000) overnight at 4°C. After washing three times with TBS-T, the membrane was stained with anti-rabbit IgG (1:10 000) for 1 h. Blots were washed (as described above) and developed using SuperSignal™ West Pico PLUS Chemiluminescent Substrate (ThermoScientific, Singapore) and visualized using the G:Box chemi imaging system (Syngene). Protein expression levels were normalized to GAPDH (Cell Signalling, 1:10 000) or α-tubulin (abcam, 1:10 000).

Quantitative reverse transcription polymerase chain reaction

Total RNA was extracted from cultured cells using the High Pure RNA Extraction kit (Roche) according to manufacturers' instructions. Total RNA was extracted from homogenized tissue using Fibrous Tissue RNeasy minikit (Qiagen). Subsequently, 1 μg DNase-free RNA was reverse transcribed using the High Capacity cDNA Reverse Transcription Kit (Thermo Fisher Scientific).

Quantitative reverse transcription polymerase chain reaction (qRT-PCR) was carried out using fluorescent SYBR Green (Roche). Primers were designed using PrimerBlast (exon and intron spanning when possible) with the following sequences. Human *ITGBL1*: F 5′-CCATCTCTGAGGCCATGGTA-3′, R 5′-ACACAAGTCCACTTCCATCTGA-3′; porcine *Itgbl1*: F 5′-CTTTGCTCGGGGAAGGGTTC-3′, R 5′-TCCATCCATCCCAGCATTCG-3′; murine *Itgbl1*: F 5′-CATCTGCTCCAATGCAGGTACA-3′, R 5′-GCTTTCCCATGGGGTGATGT-3′. Porcine collagen 1 alpha 1 (*col1a1*): F 5′-TCACGTCATCGCACAACACA-3′, R 5′-GAAGCGATGGTGGGATTGAG-3′; murine *Col1a1*: F 5′-GGTAACGATGGTGCTGTTGG-3′, R 5′-GGGACCTTCAGAGCCTCTAG-3′. Human β2Microglobulin (*B2M*): F 5′-AGATGAGTATGGCTGCCGTG-3′, R 5′-GCGGCATCTTCAAACCTCCA-3′, porcine *B2m*: F 5′- CAAGATAGTTAAGTGGGATCGAGA-3′, R 5′- TGGTAACATCAATACGATTTCTGA-3′, murine *B2m*: F 5′-CTGACCGGCCTGTATGCTA-3′, R 5′-CAGTCTCAGTGGGGGTGAAT-3′. Porcine TATA box binding protein (*Tbp*): F 5′-GGGAGAGCTCTGGGATTGTG-3′, R 5′-AGCAGCAAATCGCTTGGGA-3′, murine *Tbp*: F 5′-ACGGTGAATCTTGGGCTGTAAAC-3′, R 5′-GCAGCAAATCGCTTGGGATTA-3′. Ct values were measured using a LightCycler 480 sequence detector (Roche). Relative fold change in gene expression was calculated with the ΔΔCT method, expression of *B2M* and/or *TBP* were used as endogenous controls for normalization.

Pyrosequencing

Genomic DNA isolated from human cardiac tissue and from HCFs treated with 5 ng/mL TGF-β1 or vehicle control, was bisulfite converted using the EZ DNA Methylation-Lightning Kit (Zymo) according to manufacturer's instructions. Specific amplification of bisulfite converted gDNA and pyrosequencing were carried out at the Genomics Core Facility, Ulster University. The primers used for human *ITGBL1* were designed to assess methylation at CpG sites within the 500 bp region of interest identified in the methylation sequencing. Primer assays were designed using PyroMark Assay Design SW 2.0. Primers used were F GGTGTGATAAGTTATTGGTTTAAATAGT, R AAAAAACCTTTAAAATAATCCCTAAAT, S GGTTTAAATAGTTGGAAGTATG, and the sequence to analyse was ATAYGTTTTTTAAAGATTAAAGAAATGAAATATTTAGTTTAAATTAAAGGATA

ATAAATGTAAGAAAAAGTTGTGTTTGTTAGATTTTTTTGTTTYGGT TTTAATTTAAATTTTAAAGAGTGTATTTATTTTAAAAGYGTGTGGT GAAAGTAATTTTTTATTT.

Statistical analysis

All statistical analyses were performed using R (3.6.3) and GraphPad Prism software (Version 9). For *in vivo* and *in vitro* analyses, normality was assessed using the Kolmogorov–Smirnov test, with Gaussian distributed data represented as mean and standard deviation of the mean (*SD*) while non-normally distributed data are presented as median and inter-quartile range. Two-sided, unpaired Student's *t*-test was used for two-group comparison (normal distribution). Paired *t*-test was used for single tissue, different location group comparison. For non-normally distributed data, a Mann–Whitney *U* test was used. For normally distributed data in a more than two-group comparison, an ordinary one-way ANOVA test, followed by Tukey's multiple comparisons test was used. Values of $P < 0.05$ were accepted as statistically significant.

Results

The gene integrin beta-like 1 (*ITGBL1*) is identified as being up-regulated and hypomethylated in HF with IHD

Principal component analysis (PCA) was carried out on datasets generated from RNA sequencing; scatter plots comparing three principal components showed that there was sufficient separation of experimental groups, NF versus HF with IHD, within RNA sequences (*Figure* 1A). Following differential gene expression analysis, a volcano plot was created plotting genes that had a fold change of >2 or <-2 and a false discovery rate adjusted *P* value of >0.05; there were 109 significantly up-regulated genes and 96 down-regulated genes in HF with IHD patients versus NF controls. The complete list of differentially expressed genes is outlined in *Table* S2. The gene *ITGBL1* is highlighted on this volcano plot as up-regulated, with a fold change of 2.205 (*adj P* = 0.03*) (*Figure* 1B).

In the methylation sequencing carried out previously, a total of 62 678,500 bp-long differentially methylated regions (DMRs) were analysed for altered methylation in human cardiac tissue.[7] A difference in methylation of ≥10% at 5× coverage with a 5% false discovery rate in the HF with IHD patient group when compared with the NF control group were considered for further analysis. A volcano plot was generated to display genes that were hypomethylated and hypermethylated in HF with IHD cardiac tissue in comparison with NF controls. There were 54 unique DMRs identified in the HF with IHD patients versus the NF controls; 9 hypermethylated and 45 hypomethylated. The complete list of differentially methylated genes is outlined in *Table* S3. *ITGBL1* was significantly hypomethylated with a percent methylation difference of 10.513 (*adj P* = 0.01*) in HF with IHD compared with NF (*Figure* 1C).

ITGBL1 was one of four genes identified as both significantly up-regulated and significantly hypomethylated in HF with IHD compared with NF controls, which were selected as genes of interest for further validation. Investigation on the other three genes of interest is ongoing. Results of our comparative analysis of RNA sequencing and methylation sequencing carried out on HF with IHD versus NF IVS tissue is summarized in a Venn diagram (*Figure* 1D). Differential gene expression and methylation analysis results, including FDR adjusted *P* value and fold change/% difference in expression/methylation, of *ITGBL1* in HF with IHD LV tissue compared with NF controls are outlined in tables (*Figure* 1E).

Verification that expression of *ITGBL1* is increased and hypomethylated in HF with IHD

Gene expression of *ITGBL1* was measured using qRT-PCR in the IVS tissue from HF with IHD (*n* = 9) patients and NF (*n* = 9) patients to verify that this gene was differentially expressed. There was significantly higher expression of *ITGBL1* in HF with IHD patient tissue RNA samples in comparison with NF controls (*P* = 0.0029**, *Figure* 2A). Furthermore, western blotting analysis was carried out on protein isolated from tissue from these matching patient samples wherein ITGBL1 was measured and visualized on protein membranes (*Figure* 2B) followed by densitometry analysis. In alignment with the gene expression analysis, we observed significantly higher levels of ITGBL1 protein in HF with IHD tissue samples in comparison with NF controls (*P* = 0.0378*, *Figure* 2C). Expression of *ITGBL1* was correlated with LVEF measured by echocardiography in the 18 patients included in this study cohort, there was a significant negative correlation between *ITGBL1* relative expression and LVEF ($r = -0.6367$, *P* = 0.0094**, *Figure* 2D).

Levels of CpG methylation were assessed within the 500 bp region of predicted DMR of the *ITGBL1* DNA sequence, as identified in the methylation sequencing, to verify that this gene is hypomethylated in HF with IHD. Percentage methylation was measured in bisulfite converted genomic DNA from nine HF with IHD patients versus nine NF patients using pyrosequencing. We confirmed that there was significantly less methylation occurring in genomic DNA from HF with IHD patients in comparison with NF control patients within the 500 bp region of interest in the *ITGBL1* DNA sequence (*P* = 0.0011**, *Figure* 2E), which was indeed consistent with the methylation sequencing results. Levels of

Figure 1 *ITGBL1* identified as up-regulated and hypomethylated in HF with IHD aetiology. RNA sequencing analysis and targeted methylation sequencing analysis was carried out on human ventricular septal tissue from HF with IHD patients (n = 9) and NF patients (n = 9). (A) Principal component analysis plot depicting separation of experimental groups by patterns of gene expression principal components. (B) Volcano plot outlining significant up-regulated (red) and down-regulated (blue) genes in HF with IHD LV tissue compared with NF controls. *ITGBL1* is highlighted. (C) Volcano plot outlining significant hypermethylated (red) and hypomethylated (blue) genes in HF with IHD LV tissue compared with NF controls. *ITGBL1* is highlighted. (D) Venn diagram illustrating differential gene expression profiles and differential methylation profiles in HF with IHD LV tissue compared with NF controls. Identification of *ITGBL1* as a gene of interest is highlighted in red. (E) Tables showing results of differential gene expression analysis and differential methylation analysis FDR adjusted *P* value and fold change/% difference in expression/methylation of *ITGBL1* in HF with IHD LV tissue compared with NF controls. HF, heart failure; IHD, ischemic heart disease; LV, left ventricle/left ventricular; NF, non-heart failure.

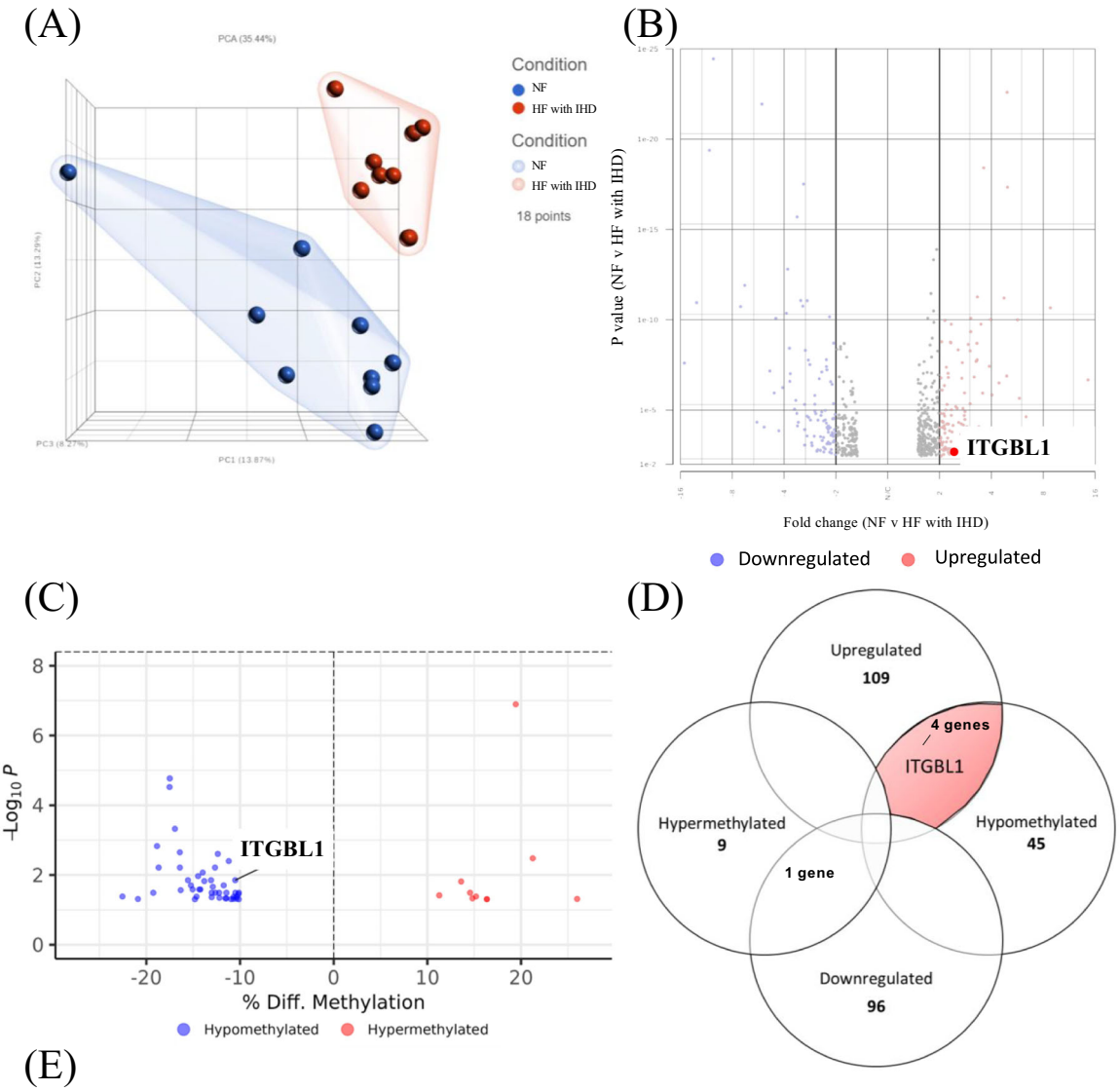

(E)

Gene symbol	Gene name	FDR adjusted p-value	Fold change	Expression status
ITGBL1	integrin subunit beta like 1	0.03	2.205	Up-regulated

Gene symbol	Gene name	FDR adjusted p-value	% methylation difference	Expression status
ITGBL1	integrin subunit beta like 1	0.01	-10.513	Hypomethylated

Figure 2 Validation that *ITGBL1* expression is increased in HF with IHD, correlates with reduced EF and is hypomethylated. (A) RT-PCR analysis of *ITGBL1* in human LV tissue from HF with IHD patients (n = 9) and NF control patients (n = 9); *B2M* expression used as reference gene. (B) Western blotting representative images of ITGBL1 and GAPDH protein levels in HF with IHD (n = 4) and NF (n = 4) LV tissue. (C) Densitometry analysis of western blotting on HF with IHD human LV tissue (n = 9) compared with NF controls (n = 9); GAPDH used as a reference protein. (D) Correlation between *ITGBL1* expression and % ejection fraction in HF with IHD patients (n = 9) and NF control patients (n = 9). (E) Percentage of methylation within a 500 bp region of predicted differential methylation on the *ITGBL1* DNA sequence in genomic DNA from human LV tissue from HF with IHD patients (n = 9) and NF control patients (n = 9) measured by pyrosequencing. (F) Correlation between *ITGBL1* expression and percentage CpG methylation within the identified 500 bp region of predicted hypomethylation on the *ITGBL1* DNA sequence in HF with IHD patients (n = 9) and NF control patients (n = 9). HF, heart failure; IHD, ischemic heart disease; LV, left ventricle/left ventricular; NF, non-heart failure.

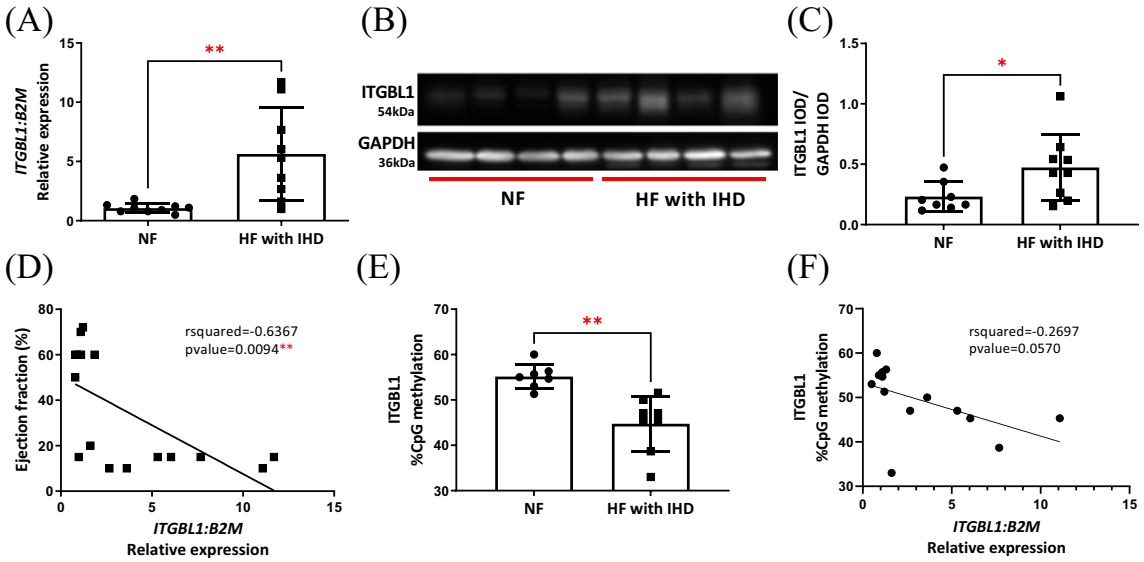

percentage CpG methylation in the *ITGBL1* sequence were correlated to gene expression of *ITGBL1*; there was a negative correlation between *ITGBL1* methylation and *ITGBL1* expression (r = −0.2697, P = 0.0570*, *Figure* 2F).

Itgbl1 is increased in both a porcine model and a murine model of myocardial ischaemia, and correlates with diminished cardiac function

To validate that *Itgbl1* was differentially expressed in myocardial ischaemia, we utilized a porcine model of ischaemia-reperfusion and a murine model of myocardial infarction.

Expression of *Itgbl1* was significantly increased in cardiac scar tissue from pigs that underwent ischaemia-reperfusion in comparison with both remote tissue from the hearts of the same pigs that underwent the procedure, and from healthy control pigs that did not undergo any procedure (P = 0.0037***, *Figure* 3A). Itgbl1 protein levels in matching tissue from the pigs subjected to this model was measured via western blotting technique (*Figure* 3B), results of densitometry analysis on these western blots shows that there were significantly higher levels of protein in the scar region of the hearts in the ischaemia-reperfusion pigs in comparison with matching remote tissue from the animals and heart tissue from healthy control animals (P = 0.0032**, *Figure* 3C). Correlation analysis was carried out to compare *Itgbl1* expression with LVEF from pigs that underwent ischaemia-reperfusion and healthy control pigs. There was a significant negative correlation between *Itgbl1* expression and LVEF in these animals (r = −0.6885 P = 0.0093**, *Figure* 3D). Increased collagen production and deposition is indicative of augmented scar tissue formation and therefore reflects the level of cardiac fibrosis occurring within the tissue.[5] Correlation analysis was also carried out to compare *Itgbl1* expression with collagen deposition measured via positive pixel analysis of picrosirius red stained LV tissue and *Col1a1* expression in LV tissue from pigs that underwent ischaemia-reperfusion and healthy control pigs. There was a significant positive correlation between *Itgbl1* expression and collagen deposition (r = 0.6879, P = 0.0406*, *Figure* 3E), and between *Itgbl1* expression and *Col1a1* expression (r = 0.6285, P = 0.0008***, *Figure* 3F) in these animals.

Itgbl1 gene expression measured by qRT-PCR was also significantly higher in mice that underwent experimental MI via coronary artery ligation versus control mice that underwent sham surgery (P = 0.0317*, *Figure* 3G). Western blotting analysis carried out on matching LV tissue from these animals showed visibly increased levels of Itgbl1 protein in mice that experienced myocardial infarction in comparison with sham controls (*Figure* 3H). This difference was quantitatively assessed using densitometry to show the increase in LV Itgbl1

Figure 3 In two animal models of ischaemia, increased *Itgbl1* correlates with reduced EF and increased fibrosis. (A) RT-PCR analysis of *Itgbl1* in LV scar tissue from pigs that underwent balloon angioplasty/reperfusion procedure (I/R) (n = 8), compared with LV remote tissue from the same animals (remote) and control animals that did not undergo surgery (control) (n = 5). (B) Western blotting representative images of Itgbl1 and α-tubulin protein levels in tissue from control pigs and remote tissue and scar tissue from I/R pigs (n = 4 per group). (C) Densitometry analysis of western blotting on control pig tissue (n = 5), and remote tissue and scar tissue from I/R pigs (n = 8); α-tubulin used as a reference protein. (D) Correlation between *Itgbl1* expression and (D) % ejection fraction (n = 13), (E) % positive pixels measured in picrosirius red stained tissue (n = 9) and (F) *Col1a1* expression (n = 13) in I/R pigs and control pigs. (G) RT-PCR analysis of *Itgbl1* in LV tissue from mice that underwent myocardial infarction (MI) surgery, compared with LV tissue from control animals that underwent sham surgery (sham) (n = 5 per group). (H) Western blotting representative images of Itgbl1 and Gadph protein levels in LV tissue from MI mice and sham mice (n = 5 per group). (I) Densitometry analysis of western blotting on LV tissue from MI mice and sham mice (n = 5 per group); GAPDH used as a reference protein. Correlation between *Itgbl1* expression and (J) % ejection fraction (n = 4 per group), (K) % positive pixels measured in picrosirius red stained tissue (n = 5 per group) and (L) *Col1a1* expression in MI mice and sham mice (n = 5 per group). Geometric mean of *B2m* and *Tbp* expression used as reference for expression analysis. LV, left ventricle/left ventricular; RT-PCR, reverse transcription polymerase chain reaction.

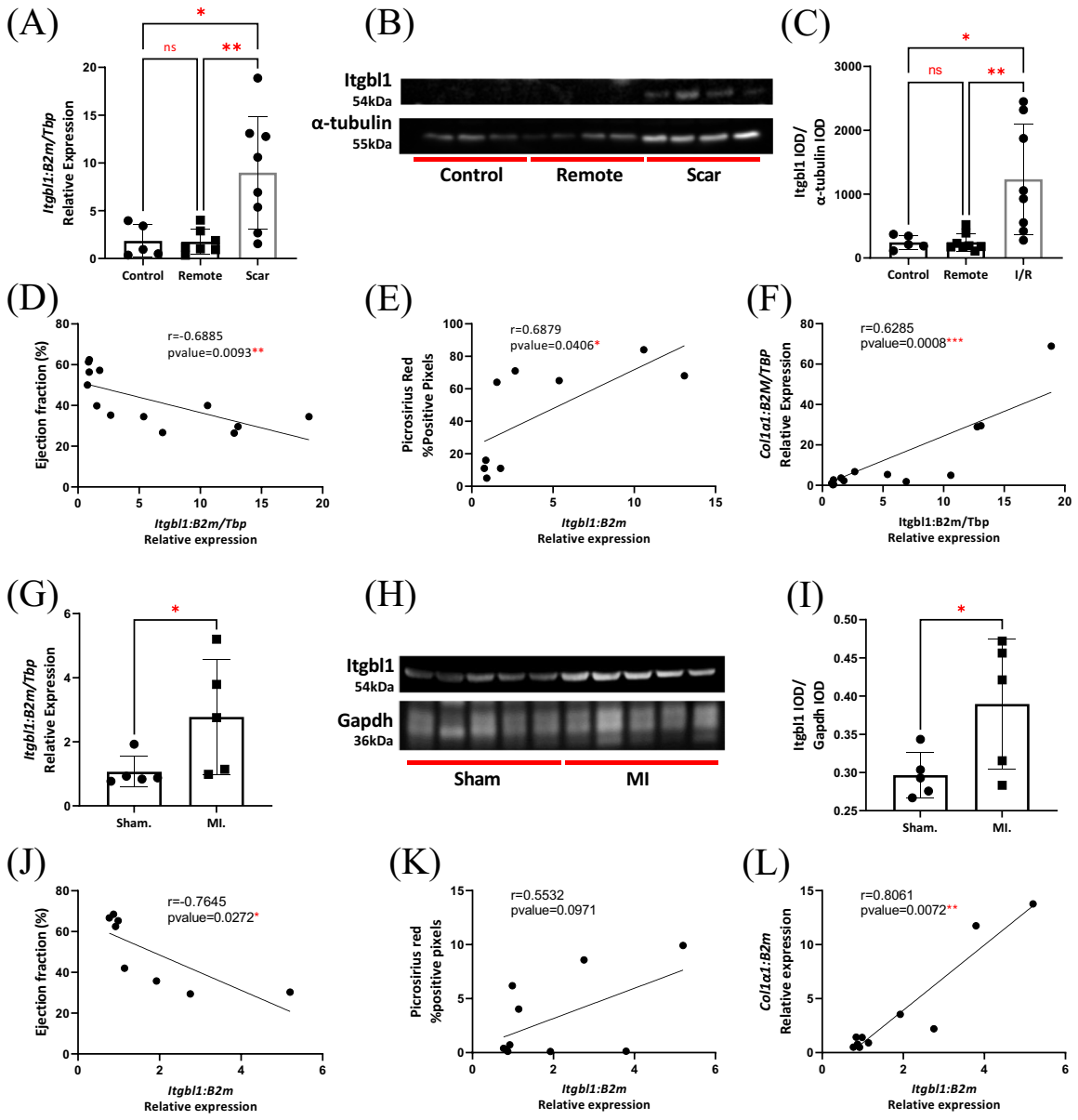

protein is statistically significant (P = 0.0498*, *Figure* 3I). *Itgbl1* relative expression also correlated negatively with LVEF in this murine model of cardiac ischaemia (r = −0.7645, P = 0.0272*, *Figure* 3J). Correlation analysis comparing *Itgbl1* expression with collagen deposition measured via positive pixel analysis of picrosirius red stained LV tissue and *col1a1*

expression was carried out on LV tissue from mice that underwent coronary artery ligation and sham-surgery control mice. There was a non-significant but positive trend between *Itgbl1* expression and collagen deposition (r = 0.5532, P = 0.0971, *Figure* 3K), and a significant correlation between *Itgbl1* expression and *Col1a1* expression (r = 0.8061, P = 0.0072**, *Figure* 3L) in these animals.

Itgbl1 is increased in a murine model of hypertension and correlates with thickening of the left ventricle and fibrosis

We assessed the expression status of *Itgbl1* in excised LV tissue collected in an Ang II-induced hypertension mouse model. Mice received 1.5 mg/kg/day Ang II via osmotic minipump (Ang II) and were compared with mice that received saline vehicle (Saline), over a total period of 4 weeks. Systolic blood pressure was significantly increased in mice that received Ang II compared with control mice that received saline ($P \leq 0.0001$***, *Figure* 4A). qRT-PCR analysis revealed that there is significantly higher expression of *Itgbl1* in Ang II hypertensive mice versus saline control mice (P = 0.0013**, *Figure* 4B). Expression of *Itgbl1* correlated positively with both IVRT (r = 0.6454, P = 0.0172*, *Figure* 4C), and LVPW (r = 0.6439, P = 0.0129*, *Figure* 4D), as measured by echocardiogram; parameters that can be indicative of LV hypertrophy and fibrosis contributing to diastolic dysfunction. We also compared *Itgbl1* expression to interstitial collagen deposition in the LV measured by positive pixel image analysis carried out on picrosirius red stained LV tissue sections and found there was a positive correlation between LV *Itgbl1* expression and LV collagen deposition (r = 0.4281, P = 0.0152*, *Figure* 4E).

Itgbl1 is primarily expressed in murine cardiac fibroblasts

10× Genomics single-nuclei RNA sequencing was performed on nuclei suspensions generated from LV tissue collected from Ang II-induced hypertensive mice, versus saline treated mice. Unsupervised clustering and marker gene detection was performed to annotate the cardiac cellular diversity of the model, according to expression of canonical cell type marker genes.

Fibroblasts and endothelial cells were the most prevalent cell populations in the nuclei isolates, with the presence of CMs, pericytes, smooth muscle cells, epicardial cells, endocardial cells, Schwann cells, B cells and NK cells, T cells, macrophages and neutrophils also being identified (*Figure* 4F). Expression of *Itgbl1* was assessed in each cell population, with the greatest expression detected in CFs, followed by a population of endocardial cells (*Figure* 4G). When *Itgbl1* expression was analysed within the CF population specifically, comparing fibroblasts from Ang II-treated mice with saline control mice, expression of *Itgbl1* was significantly increased (*log2FC* = 0.655, P = *3e-07****, *Figure* 4H). Moreover, *Itgbl1* was expressed in 53% of CFs in Ang II-treated mice versus 27% of fibroblasts in saline control mice. Correlation analysis was carried out in the CF cell population between *Itgbl1* and all other expressed genes. This generated a list of 362 genes showing significant co-expression correlation with *Itgbl1*, ranked from 'most positive' to 'most negative' correlation (*Table* S4). Gene enrichment pathway analysis was then performed using the NCATS BioPlanet® database via EnrichR using genes that positively correlated with *Itgbl1* expression (*Table* S5). The top 10 pathways identified as enriched with *Itgbl1*-correlated genes in CFs are illustrated in *Figure* 4I.

ITGBL1 expression is induced and hypomethylated in activated human cardiac fibroblasts and is important for fibroblast migration

To investigate the role of *ITGBL1* in CFs, we first measured *ITGBL1* expression in HCFs that had been activated, either via exposure to hypoxic conditions (cells cultured at 1% oxygen versus cells cultured at 21% oxygen for 48 h), or via treatment with 5 ng/mL TGF-β1 for 24 h. We showed that there is increased *ITGBL1* expression in hypoxic HCFs compared with healthy normoxic HCFs (P = 0.0226*, *Figure* 5A), and in TGF-β1 treated HCFs compared with healthy control HCFs ($P \leq 0.0001$***, *Figure* 5B). As fibroblasts are also activated by factors secreted from CMs in response to stress or injury,[11] the effect of conditioned media collected from AC16s treated with 25 nM Ang II on HCF *ITGBL1* gene expression was examined. A significant increase in *ITGBL1* expression was observed in HCFs cultured in the myocyte Ang II conditioned media in comparison with cells cultured in the myocyte control and cell free Ang II conditioned media (P = 0.0344*, *Figure* 5C).

To assess the functional impact of *ITGBL1* expression in CFs, *ITGBL1*-targeted siRNA gene knockdown was used. A significant knockdown of *ITGBL1* gene expression in HCF cells was observed when transfected with 20 nM siRNA for 48 h (siRNA), compared with cells transfected with a scrambled control (scr) (P = 0.0091**, *Figure* 5D). The cell migration potential of HCFs transfected with *ITGBL1* siRNA was assessed via a wound closure assay. A significant reduction in wound closure was detected in cells transfected with the *ITGBL1* siRNA compared with scrambled control, 24 h following wound creation (P = 0.0005***, *Figure* 5E,F).

To determine whether the increased expression of *ITGBL1* is mediated by hypomethylation of the *ITGBL1* DNA sequence, pyrosequencing was conducted. Total CpG methylation within the 500 bp DMR, in accordance with the human

Figure 4 Itgbl1 is increased in hypertensive mice, correlates with LV thickening/fibrosis, and is specifically expressed in CFs. (A) Systolic blood pressure (mmHg) measured in mice that received 1.5 mg/kg/day angiotensin-II via minipump for 28 days (Ang II) compared with mice that received saline (saline) (n = 7 per group). (B) RT-PCR analysis of *Itgbl1* in LV tissue from Ang II-infused mice compared with mice that received saline (n = 7 per group); *B2m* expression was used as reference. Correlation between *Itgbl1* expression and (C) isovolumic relaxation time (IVRT) (ms), (D) LV posterior wall thickness in diastole (LVPW;d) and (E) % positive pixels in LV tissue stained with picrosirius red in Ang II-infused mice (n = 7) and mice that received saline (n = 6). (F) UMAP of heart cell populations annotated by expression of canonical cell type markers. (G) *Itgbl1* is primarily expressed in the fibroblasts, in addition to the less numerous endocardial population. (H) Expression of *Itgbl1* is up-regulated in fibroblasts from Ang II-infused mice compared with fibroblasts from mice that received saline (log2FC = 0.65, P = 0.00087). (I) Top 10 cell pathways identified as being associated with genes significantly correlating with *Itgbl1* expression; gene enrichment pathway analysis performed using NCATS BioPlanet® software on 350 genes expressed in cardiac fibroblasts from Ang II-infused mice, using a cut-off of positive correlation >0.15 tau and sorted by adj pval. HF, heart failure; LV, left ventricle/left ventricular; RT-PCR, reverse transcription polymerase chain reaction.

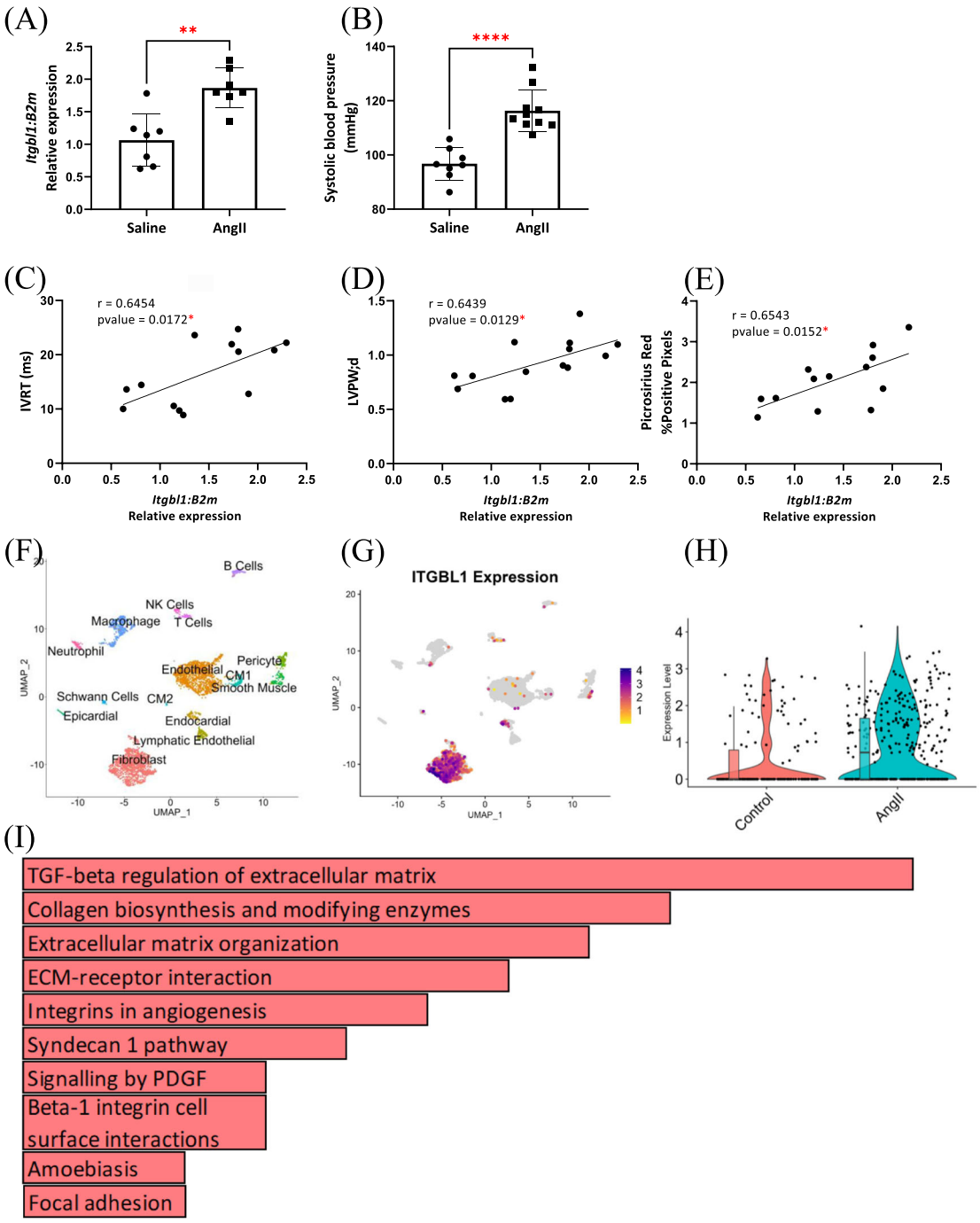

Figure 5 *ITGBL1* expression is induced in stimulated human CFs, is important for migration and is hypomethylated. RT-PCR analysis of *ITGBL1* in human ventricular cardiac fibroblasts (HCFs) (A) exposed to 1% oxygen (compared with 21% normoxia) for 48 h (n = 5 per group), (B) treated with 5 ng TGF-β1 (or vehicle control) for 24 h (n = 5 per group) and (C) cultured in supernatants collected from Ac16 myocytes treated with 25 nM Angiotensin II for 72 h (compared with Ac16 media containing 25 nM angiotensin-II or supernatants from untreated Ac16 myocytes) for 24 h (n = 4 per group). (D) RT-PCR analysis of *ITGBL1* in HCFs transfected with 20 nM *ITGBL1* siRNA (or empty vector lentivirus) (n = 4 per group). Migration assays were performed to investigate migratory abilities of HCF cells; (E) % wound closure was calculated in cells transfected with *ITGBL1* siRNA (or scrambled control) (n = 4 per group), (F) representative images of migration assays at 24 h wound closure. (G) Percentage of methylation within a 500 bp region of predicted differential methylation on the *ITGBL1* DNA sequence in genomic DNA from HCFs treated with 5 ng TGF-β1 compared with untreated HCFs measured by pyrosequencing (n = 5 per group). (H) Correlation between *ITGBL1* expression and *ITGBL1* percentage CpG methylation in genomic DNA from HCFs treated with TGF-β1 compared with untreated HCFs (n = 5 per group). CF, cardiac fibroblasts; HCF, human CF; HF, heart failure; LV, left ventricle/left ventricular; RT-PCR, reverse transcription polymerase chain reaction.

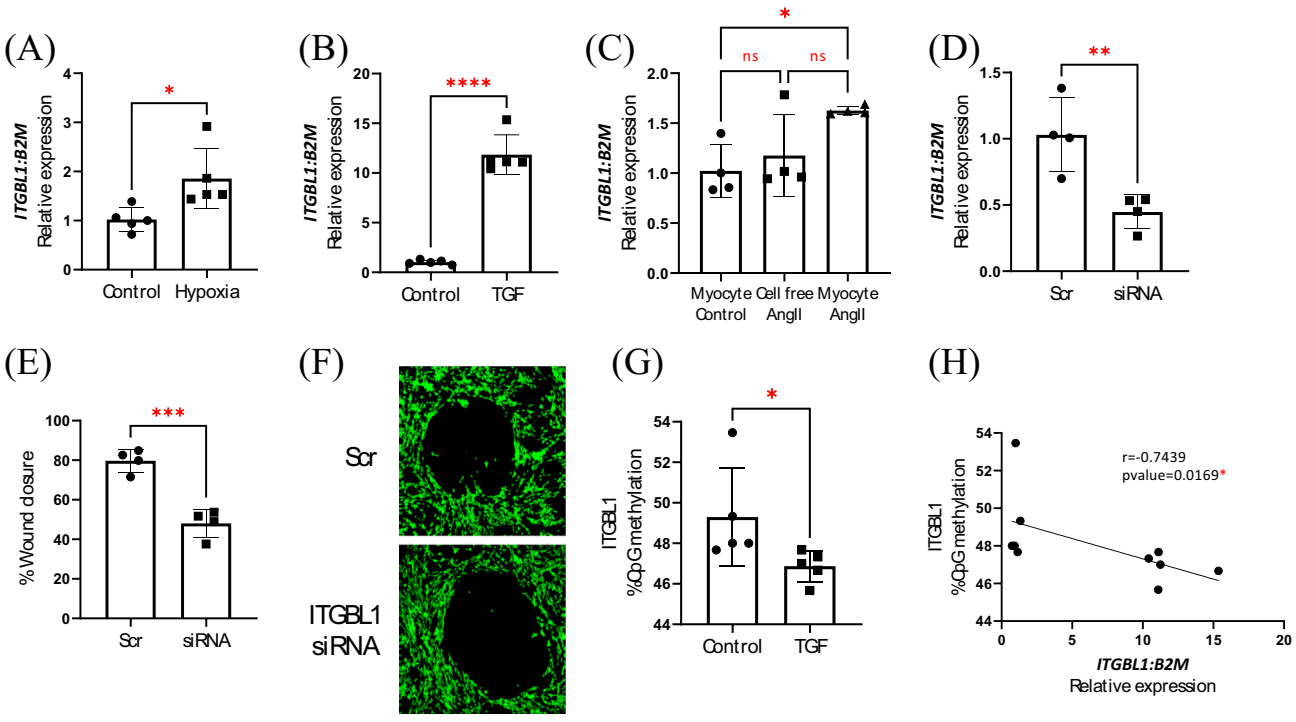

cardiac tissue methylation sequencing results, on the *ITGBL1* DNA sequence was quantified in HCFs stimulated with 5 ng/mL TGF-β1 for 24 h. A significant reduction in methylation was detected on the *ITGBL1* gene in TGF-β1-treated cells compared with controls (P = 0.0159*, *Figure* 5G). There was also a significant negative correlation between *ITGBL1* CpG methylation and *ITGBL1* expression in HCF cells stimulated with TGF-β1 compared with controls (r = −0.7439, P = 0.0169*, *Figure* 5H).

Discussion

Despite HF with IHD being the most common cause of HF in the developed world, there is an overall lack of understanding behind cell specific molecular alterations that contribute to disease development. Therefore, addressing the gap of knowledge would ultimately enable the development of novel biomarkers and therapeutics for HF with IHD patients. Alterations in epigenetic regulation, such as DNA methylation, can result in widespread differential gene expression. There is an increasing understanding of global DNA methylation changes within cardiac tissue in HF[7,12]; however, few studies have attempted to identify cell specific, DNA methylation sensitive genes that play a role in HF with IHD.

In this study, we carried out a comparative analysis of RNA sequencing and bisulfite methylation sequencing on LV septal tissue from a cohort of HF patients with IHD aetiology and a matched cohort of NF patients. This analysis identified *ITGBL1* as a gene of interest, as this gene was found to be up-regulated and hypomethylated in HF with IHD LV tissue when compared with NF controls. ITGBL1 encodes a peptide similar to the structure of integrin beta subunits but it has been suggested that this peptide does not function in the same way as other integrins due to its lack of an Arg-Gly-Asp-binding domain or transmembrane domain.[13,14] *ITGBL1*

was first cloned and characterized from foetal lung, HUVEC and osteoblast cDNA libraries in which a sequence encoding a peptide similar to the cysteine-rich 'stalk-like' structure of integrin beta subunits was identified.[13] *ITGBL1* has been shown to mediate bone cancer metastasis in breast cancer patients,[15] and others have reported that it is involved in converting lung fibroblasts to activated myofibroblast-like cells in primary colorectal cancer metastatic growth.[16]

This study validated that *ITGBL1* is up-regulated in LV cardiac tissue from HF patients with evidence of IHD in a range of animal models of cardiac ischaemia. Both gene expression and protein levels of ITGBL1 were found to be increased in LV scar tissue excised from a pig ischaemia-reperfusion model, in LV tissue from a mouse model of experimental MI and in a mouse model of Ang II-induced hypertension. Interestingly, this data also showed that *ITGBL1* gene expression correlated with reduced LVEF in both the human patient cohort and in the animal models of ischaemia, and correlated with LV thickening and fibrosis in the animal hypertension model. This data complements findings in a recent 2023 study in which *Itgbl1* expression was assessed in an animal model of TAC pressure-overload, wherein *Itgbl1* expression was significantly increased and *Itgbl1* knockdown alleviated LV wall thickness and improved LVEF in TAC-operated mice.[17] Chen et al analysed online datasets from the Gene Expression Omnibus (GEO) database and found that *ITGBL1* was elevated in DCM, HF with IHD and diabetic HF patients in comparison with normal hearts.[17] *ITGBL1* was also shown to be up-regulated at the gene level in a multi-omics analysis of DCM cardiac tissue,[18] however this current study is the first to carry out a robust assessment of RNA and protein expression levels of ITGBL1 in human cardiac tissue and expound on the association between ITGBL1 and vital cardiac function parameters. This work was expanded into the novel assessment of Itgbl1 levels in the context of *in vivo* myocardial infarction and Ang II-induced hypertension.

Single nuclei RNA sequencing was carried out on LV tissue collected from Ang II-induced hypertensive mice, which enabled investigation of cell type specific *Itgbl1* expression within the heart. This study reports that *Itgbl1* is primarily expressed in CFs, with expression also being detected in a small population of endocardial cells. Evidence presented in other studies show that there is greater *Itgbl1* expression in mouse and rat CFs when compared with CMs *in vitro*[17] and that the expression of *Itgbl1* was higher in CFs isolated from the hearts of adult mice compared with CMs.[17] This study confirmed that *Itgbl1* expression was increased in fibroblasts from Ang II-treated mice compared with controls and identified that genes significantly correlating with *Itgbl1* in this cell population are enriched in cell pathways associated with cardiac fibrosis, including regulation and organisation of the extracellular matrix (ECM), and collagen biosynthesis. These data culminate with findings in which *Itgbl1* was observed to be associated with pro-fibrotic genes, such as connective tissue growth factor (CTGF), postn, col8a1, cilp and sperpine1.[17] It was therefore postulated that ITGBL1 could have a role in the function of CFs.

This study aimed to reveal the stimuli likely causative for the increase in *ITGBL1* expression in human CFs and elucidate what effect *ITGBL1* has on fibroblast migratory function. Other studies have shown that TGF-β1 treatment stimulates *Itgbl1* expression in neonatal rat CFs.[19] Our gene enrichment pathway analysis on genes correlating with *Itgbl1* also indicated it may be strongly associated with TGF-β1 regulation of ECM. Findings in this study showed that CF expression of *ITGBL1* can be induced by exposure to a hypoxic environment and by treatment with TGF-β1; tissue hypoxia and increased cell secretion of TGF-β1 reflect the characteristics of the ischaemic heart.[20] CF *ITGBL1* expression was not induced by Ang II treatment in culture,[19] but given the increase in *Itgbl1* expression in the LV tissue from the Ang II-hypertensive model, *ITGBL1* expression in CFs could be driven by stimuli secreted by stressed CMs. CF *ITGBL1* expression was induced following exposure to conditioned media collected from Ang II-treated AC16 CMs, but not by cell-free AC16 media containing Ang II alone; this suggests that differential expression of this gene in CFs is affected not only by the general stress/injury response in the heart but also by factors secreted from local cell populations within cardiac tissue.

To assess the functional effects of deregulated *ITGBL1* expression in CFs, cell migration was investigated. *ITGBL1* gene knockdown reduced the wound closure ability of these cells, suggesting that this gene plays a role in CF migration. *Itgbl1* knockdown impacted on collagen contraction in neonatal rat CFs[17]; however, the expression of *ITGBL1* and its effect on fibroblast regulation and functionality had never been investigated in human cardiac cells until now. ITGBL1 has also been reported to be implicated in cell migration in other pathologies such as metastatic cancer.[21–23] The findings of this study further corroborate a pivotal role for ITGBL1 in the activation and migration of CFs, and emphasizes a clear significance for this gene in regard to human cardiac pathology.

ITGBL1 expression has been shown to be activated by TGF-β1 and has been implicated as an activator of TGF-β1/SMAD pathway[21,22]; studies have also indicated that *ITGBL1* is a transcriptional target of RUNX2.[23] In this current study, we identified *ITGBL1* expression is affected by dysregulated DNA methylation. Fluctuations in DNA methylation have been associated with CF activation, and it has been shown that DNA methylation in fibroblasts can be altered due to various environmental features; ranging from changes in blood pressure to changes in physical activity.[5,6] *ITGBL1* has specifically been shown to be susceptible to altered epigenetic modifications in other disease pathologies[24,25] and was found to be hypomethylated in our genome wide methylation sequencing of human cardiac tissue. This study provides evidence that *ITGBL1* is significantly hypomethylated

within a 500 bp region of predicted differential methylation, in both the HF with IHD v NF patient LV tissue and in HCFs treated with TGF-β1. It was also shown that this reduced *ITGBL1* CpG methylation correlates with increased *ITGBL1* gene expression in both the human tissue and in TGF-β1-stimulated CFs, further supporting the hypothesis that increased levels of *ITGBL1* are attributed to *ITGBL1* hypomethylation.

One of the main limitations to our study is the level of gender bias in the models utilized. Our human RNA sequencing and DNA methylation sequencing data is limited by the fact that all patients included in the sample cohort were male; hence, it was not possible to determine the effect of sex on gene expression or DNA methylation. However, given the scarcity of HF biopsy samples and the difficulty in obtaining LV tissue samples from relevant non-HF controls, it is a strength that our cohort included a good representation of the HF with IHD aetiology as well as non-failure controls. We were also limited in the sex of animals used in the various animal models presented in this study. Male mice do not present with an effective phenotypic myocardial infarction following coronary artery ligation comparative with females; therefore, we only used female mice for the MI model. In accordance with the three Rs of animal use, the un-used male offspring from the MI study were then used in the Ang II-induced hypertension model to reduce the number of animals used. Only male large pigs were used in the porcine model of ischaemic reperfusion as the females were used for breeding purposes. Hence, we are unable to account for sex differences in the animal models presented. This is especially important given the known impact of the female sex hormone oestrogen on the development of HF[26] and the TGF-β1 signalling pathway,[27] so it could therefore potentially influence the results depending on the animal's sex cycle. Further investigation would be required to elucidate male–female differences on *ITGBL1* expression and methylation, possibly with more in-depth optimization of animal model protocols.

In summary, the data presented in this study provide evidence that the *ITGBL1* gene is up-regulated in HF with IHD. We assessed the expression status of this gene in human cardiac LV tissue and in three different animal models of cardiac dysfunction; a porcine model of ischaemia-reperfusion, a murine model of experimental MI, and a murine model of Ang II-induced hypertension. Moreover, having confirmed that *ITGBL1* expression is consistently induced in the injured heart we have shown that *ITGBL1* expression is strongly associated with diminished LV function. We discovered, via single nuclei RNA sequencing of murine LV tissue, that *Itgbl1* is primarily expressed in CFs and could play a biological role in cardiac fibrosis. We further showed that *ITGBL1* is increased in a hypoxic environment and is activated by TGF-β1, and we elucidated a role for ITGBL1 in human fibroblast migratory function. Lastly, we proposed that dysregulation of *ITGBL1* expression in the ischaemic heart is regulated by gene-specific loss of DNA methylation.

Acknowledgements

RNA sequencing was carried out by the Queen's University Belfast Genomics Core Technology Unit. Pyrosequencing was carried out by the Genomics Core Facility, Ulster University.

Conflict of interest statement

None declared.

Funding

This work was cofunded by the Heart Research UK (RG2662) and the British Heart Foundation (PG/20/10424 and PG/18/21/33599).

Consent for publication

All authors have approved the final draft of this manuscript and provided consent for publication.

Data availability statement

The datasets generated and/or analysed during the current study are not publicly available but are available from the corresponding author on reasonable request.

Supporting information

Additional supporting information may be found online in the Supporting Information section at the end of the article.

Figure S1: Systolic blood pressure is increased in mice that receive Ang II. Study endpoint systolic blood pressure measured by tail-cuff inflation in mice that are receiving 1.5 mg/kg/day angiotensin II via osmotic minipump over a four week period, compared to mice receiving saline (n = 8–10).

Table S1. Heart failure with ischaemic heart disease patient cohort demographics.

Table S2: Differentially expressed genes in NF LVS tissue versus HF with IHD LVS tissue identified via RNA sequencing and analysed using Partek Flow Genomics suite software.

Table S3: Differentially methylated regions of genomic DNA isolated from NF LVS tissue versus HF with IHD LVS tissue identified via custom-designed next generation targeted methylation sequencing.

Table S4: Gene list of significantly differentially expressed genes in cardiac fibroblasts from an Ang II-induced hypertensive mouse model that correlate with expression of ITGBL1, filtered to remove genes with adjusted pval <0.05, sorted by 'most.

Table S5: Gene list of enrichment pathway analysis performed using NCATS BioPlanet® software on 350 genes expressed in cardiac fibroblasts from an Ang II-induced hypertensive mouse model, using a cut off of positive correlation >0.15 tau and sorted by adj pval.

References

1. Arbelo E, Protonotarios A, Gimeno JR, Arbustini E, Barriales-Villa R, Basso C, *et al*. 2023 ESC guidelines for the management of cardiomyopathies: developed by the task force on the management of cardiomyopathies of the European Society of Cardiology (ESC). *Eur Heart J* 2023;**44**:3503-3626. doi:10.1093/eurheartj/ehad194
2. Mosterd A, Hoes AW. Clinical epidemiology of heart failure. *Heart* 2007;**93** Preprint at: doi:10.1136/hrt.2003.025270
3. Khan MA, Hashim MJ, Mustafa H, Baniyas MY, Al Suwaidi SKBM, AlKatheeri R, *et al*. Global epidemiology of ischemic heart disease: results from the Global Burden of Disease Study. *Cureus* 2020;**12**:e9349. doi:10.7759/cureus.9349
4. Cabac-Pogorevici I, Muk B, Rustamova Y, Kalogeropoulos A, Tzeis S, Vardas P. Ischaemic cardiomyopathy. Pathophysiological insights, diagnostic management and the roles of revascularisation and device treatment. Gaps and dilemmas in the era of advanced technology. *Eur J Heart Fail* 2020;**22** Preprint at: doi:10.1002/ejhf.1747
5. Russell-Hallinan A, Watson CJ, Baugh JA. Epigenetics of aberrant cardiac wound healing. *Compr Physiol* 2018;**8**: doi:10.1002/cphy.c170029
6. Hsu CC, Wang JS, Shyu YC, Fu TC, Juan YH, Yuan SS, *et al*. Hypermethylation of ACADVL is involved in the high-intensity interval training-associated reduction of cardiac fibrosis in heart failure patients. *J Transl Med* 2023;**21**:187. doi:10.1186/s12967-023-04032-7
7. Glezeva N, Moran B, Collier P, Moravec CS, Phelan D, Donnellan E, *et al*. Targeted DNA methylation profiling of human cardiac tissue reveals novel epigenetic traits and gene deregulation across different heart failure patient subtypes. *Circ Heart Fail* 2019;**12**:e005765. doi:10.1161/CIRCHEARTFAILURE.118.005765
8. McLellan MA, Skelly DA, Dona MSI, Squiers GT, Farrugia GE, Gaynor TL, *et al*. High-resolution transcriptomic profiling of the heart during chronic stress reveals cellular drivers of cardiac fibrosis and hypertrophy. *Circulation* 2020;**142**:1448-1463. doi:10.1161/CIRCULATIONAHA.119.045115
9. Xie Z, Bailey A, Kuleshov MV, Clarke DJB, Evangelista JE, Jenkins SL, *et al*. Gene set knowledge discovery with Enrichr. *Curr Protoc* 2021;**1**:e90. doi:10.1002/cpz1.90
10. Huang R, Grishagin I, Wang Y, Zhao T, Greene J, Obenauer JC, *et al*. The NCATS BioPlanet—an integrated platform for exploring the universe of cellular signaling pathways for toxicology, systems biology, and chemical genomics. *Front Pharmacol* 2019;**10**:445. doi:10.3389/fphar.2019.00445
11. Ren Z, Yu P, Li D, Li Z, Liao Y, Wang Y, *et al*. Single-cell reconstruction of progression trajectory reveals intervention principles in pathological cardiac hypertrophy. *Circulation* 2020;**141**:1704-1719. doi:10.1161/CIRCULATIONAHA.119.043053
12. Pepin ME, Ha CM, Crossman DK, Litovsky SH, Varambally S, Barchue JP, *et al*. Genome-wide DNA methylation encodes cardiac transcriptional reprogramming in human ischemic heart failure. *Lab Invest* 2019;**99**:371-386. doi:10.1038/s41374-018-0104-x
13. Berg RW, Leung E, Gough S, Morris C, Yao WP, Wang SX, *et al*. Cloning and characterization of a novel β integrin-related cDNA coding for the protein TIED ('ten β integrin EGF-like repeat domains') that maps to chromosome band 13q33: a divergent stand-alone integrin stalk structure. *Genomics* 1999;**56**:169-178. doi:10.1006/geno.1998.5707
14. Takagi J, Beglova N, Yalamanchili P, Blacklow SC, Springer TA. Definition of EGF-like, closely interacting modules that bear activation epitopes in integrin β subunits. *Proc Natl Acad Sci U S A* 2001;**98**:11175-11180. doi:10.1073/pnas.201420198
15. Feng Y, Li X, Sun B, Wang Y, Zhang L, Pan X, *et al*. Evidence for a transcriptional signature of breast cancer. *Breast Cancer Res Treat* 2010;**122**:65-75. doi:10.1007/s10549-009-0505-z
16. Ji Q, Zhou L, Sui H, Yang L, Wu X, Song Q, *et al*. Primary tumors release ITGBL1-rich extracellular vesicles to promote distal metastatic tumor growth through fibroblast-niche formation. *Nat Commun* 2020;**11**:1211. doi:10.1038/s41467-020-14869-x
17. Chen XQ, Li XT, Wu XY, Ding Y, Li Y, Zhou GQ, *et al*. Integrin beta-like 1 mediates fibroblast-cardiomyocyte crosstalk to promote cardiac fibrosis and hypertrophy. *Cardiovasc Res* 2023;**119**:1928-1941. doi:10.1093/cvr/cvad104
18. Portokallidou K, Dovrolis N, Ragia G, Atzemian N, Kolios G, Manolopoulos VG. Multi-omics integration to identify the genetic expression and protein signature of dilated and ischemic cardiomyopathy. *Front Cardiovasc Med* 2023;**10**:1115623. doi:10.3389/fcvm.2023.1115623
19. Wang HB, Huang R, Yang K, Xu M, Fan D, Liu MX, *et al*. Identification of differentially expressed genes and preliminary validations in cardiac pathological remodeling induced by transverse aortic constriction. *Int J Mol Med* 2019;**44**: doi:10.3892/ijmm.2019.4379
20. Watson JA, Watson CJ, Mccann A, Baugh J. Epigenetics, the epicenter of the hypoxic response. *Epigenetics* 2010; **5**:293-296. doi:10.4161/epi.5.4.11684
21. Li W, Li S, Yang J, Cui C, Yu M, Zhang Y. ITGBL1 promotes EMT, invasion and migration by activating NF-κB signaling pathway in prostate cancer. *Onco Targets Ther* 2019;**12**:10693-10701. doi:10.2147/OTT.S200082
22. Huang W, Yu D, Wang M, Han Y, Lin J, Wei D, *et al*. ITGBL1 promotes cell migration and invasion through stimulating the TGF-β signalling pathway in hepatocellular carcinoma. *Cell Prolif* 2020; **53**:e12836. doi:10.1111/cpr.12836
23. Li XQ, du X, Li DM, Kong PZ, Sun Y, Liu PF, *et al*. ITGBL1 is a Runx2 transcriptional target and promotes breast cancer bone metastasis by activating the TGFβ

signaling pathway. *Cancer Res* 2015;**75**: 3302-3313. doi:10.1158/0008-5472.CAN-15-0240
24. Gan X, Liu Z, Tong B, Zhou J. Epigenetic downregulated ITGBL1 promotes non-small cell lung cancer cell invasion through Wnt/PCP signaling. *Tumor Biol* 2016;**37**:8461. doi:10.1007/s13277-016-4834-3
25. Lian XY, Ma JC, Zhou JD, Zhang TJ, Wu DH, Deng ZQ, *et al*. Hypermethylation of ITGBL1 is associated with poor prognosis in acute myeloid leukemia. *J Cell Physiol* 2019;**234**: 9438-9446. doi:10.1002/jcp.27629
26. Khan SS, Beach LB, Yancy CW. Sex-based differences in heart failure: JACC focus seminar 7/7. *J Am Coll Cardiol* 2022;**79** Preprint at: doi:10.1016/j.jacc.2022.02.013
27. Van Eickels M, Rolf S, Doevendans PA, Meyer R, Grohé C, Schlüter KD. The influence of oestrogen-deficiency and ACE inhibition on the progression of myocardial hypertrophy in spontaneously hypertensive rats. *Eur J Heart Fail* 2005;**7**: 1079-1084. doi:10.1016/j.ejheart.2005.03.004